Analysis of Hollow Fiber Reverse Osmosis Membrane Module of Axial Flow Type

Atsuo Kumano,[1,2] Hideto Matsuyama[1]

[1]*Center for Membrane and Film Technology, Department of Chemical Science and Engineering, Kobe University 1-1 Rokkodai, Nada-ku, Kobe 867-6501, Japan*
[2]*Desalination Membrane Department, Toyobo Co., Ltd., 2-8 Dojima Hama 2-Chome, Kita-ku, Osaka 530-8230, Japan*

Received 24 May 2010; accepted 20 February 2011
DOI 10.1002/app.34404
Published online 28 July 2011 in Wiley Online Library (wileyonlinelibrary.com).

ABSTRACT: Several analyses of hollow fiber reverse osmosis (RO) modules in which permeate water flows from the outer to the inner side of the membrane have been attempted over the past 20 years. In our previous work, an FCP (Friction Concentration Polarization) model showed good agreement with a wide range of actual performance data of a hollow fiber RO membrane module of radial flow type. In this work, this analytical model was applied to axial flow type hollow fiber modules. The performance of the axial flow type module with high packing density of hollow fibers was analyzed, taking into consideration the axial concentration profile in the module. It was confirmed that this model showed good agreement with experimental data for an axial flow type RO membrane module. © 2011 Wiley Periodicals, Inc. J Appl Polym Sci 123: 463–471, 2012

Key words: membranes; modeling; calculations; reverse osmosis; axial flow type module

INTRODUCTION

The reverse osmosis (RO) separation process has become important as an energy saving process (no phase change) for brackish water and seawater desalination. Hollow fibers have been selectively employed in industry because of their economical efficiency when compared with several other membrane types.[1,2] Hollow fiber membrane modules are separated into two classes on the basis of the direction of permeated water flow, the outside-to-inside type, and inside-to-outside type modules. It is well known that outside-to-inside type modules typically have a number of advantages, such as higher effective membrane area and lower pressure loss on the feed side, compared with inside-to-outside type modules. Consequently, outside-to-inside type modules are used in typical RO membrane modules due to higher operation pressure.

Several analyses of hollow fiber RO membrane modules in which permeate water flows from the outside to the inside of the hollow fiber have been attempted over the past 20 years. Gill and Bansal[3] proposed a mathematical model in which the pressure drop inside the fiber and constant salt rejection were considered, assuming no concentration polarization. Gill et al.[4,5] improved this model by introducing the solution-diffusion model. In their work, the membrane transport model was improved based on a constant rejection model and became more realistic. Ohya et al.[6] proposed a simple and practical model by considering concentration polarization, which was neglected by other researchers. However, the pressure drop inside the fiber was ignored in this model. The transmembrane pressure was consequently overestimated, reducing the pure water permeability coefficient in the calculation. The FCP model (Friction Concentration Polarization model), in which both concentration polarization and the pressure drop inside the fiber were considered, has already been presented as an analytical model of a hollow fiber RO module, and its validity has been proven by Sekino et al. through verification with a wide range of actual performance data on a hollow fiber RO membrane module.[7,8]

In the aforementioned models hollow fiber modules of the radial flow type were analyzed, because most commercialized hollow fiber RO membrane modules are of that type, especially for seawater desalination at high pressure and brackish water desalination at medium pressure. One of the typical radial flow type modules with hollow fiber RO membranes is the cellulose triacetate hollow fiber module. The schematic structure and flow of a representative radial flow type module (HA3110; Toyobo Co.) is shown in Figure 1. The cellulose

Correspondence to: H. Matsuyama (matuyama@kobe-u.ac.jp).

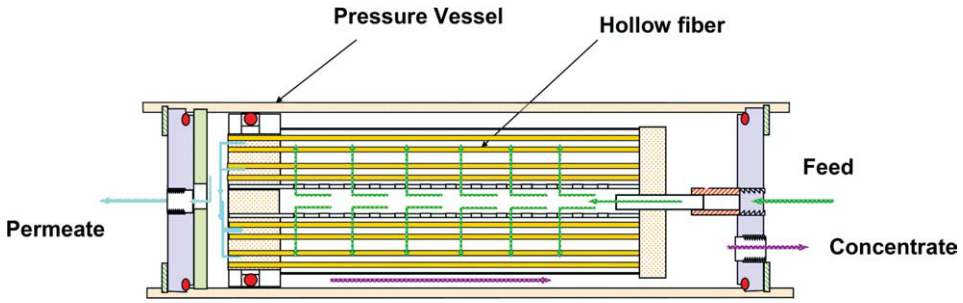

Figure 1 Schematic structure and flow pattern of typical radial flow type module. [Color figure can be viewed in the online issue, which is available at wileyonlinelibrary.com.]

triacetate hollow fibers with outer diameter 175 μm (and total number of 1×10^5 to 1×10^6 fibers) are arranged around a porous tubular core. Both ends of the cylindrical fiber bundle are potted with epoxy resin and one or both sides are then sliced vertically to give open hollow fibers. The permeation solution flows through the fiber bore to the opening. The bundle is finally inserted into a pressure vessel and sealed.

Several axial flow type RO membrane modules are used at low pressure, in addition to radial flow type modules. Recently, some axial flow type RO modules have been used, especially at low operating pressure, for purification and desalination of brackish water. The schematic structure of an axial flow type module (HK2105; Toyobo Co) is shown in Figure 2. This module with hollow fiber RO membranes is also made from cellulose triacetate hollow fibers. These hollow fibers with outer diameter 175 μm are arranged in the pressure vessel as follows. One end of the cylindrical fiber bundle is potted with epoxy resin and one side is then vertically sliced to give open hollow fibers. The permeation solution flows through the fiber bore to the opening. The bundle is finally inserted into a pressure vessel and sealed.

The axial flow type module has the advantages of higher flow velocity on the shell side of the module than is obtained in radial flow type modules. Thus, the axial flow modules operate stably and maintain highly efficient RO performance, even at unusually high recovery.

Although an analytical model (FCP model) for axial flow hollow fiber RO membrane module was published by Sekino et al.,[9] the module that was analyzed had much lower hollow fiber packing density (about 1%) than that (>50%) of practical modules, and neglected the axial concentration profile in the module.

In this study, we analyze the RO performance of the axial flow type hollow fiber module with high packing density of hollow fibers, taking into account the axial concentration profile in the module. The mass transfer correlations for an axial flow type hollow fiber module were derived, and the validity of the model was confirmed by comparing with experimental data.

Analysis

FCP model for axial flow type module

The FCP model was the first analytical model of a hollow fiber RO membrane module in which the pressure loss inside the hollow fiber was taken into account by the Kimura-Sourirajan membrane transport equation.[10] A schematic diagram of the FCP model for the radial flow type module is shown in Figure 3. The model is composed of a series of differential equations which consist of permeate flow equations in a hollow fiber, feed flow equations and so on. In this model, the mass transfer coefficient k was estimated by the following dimensionless

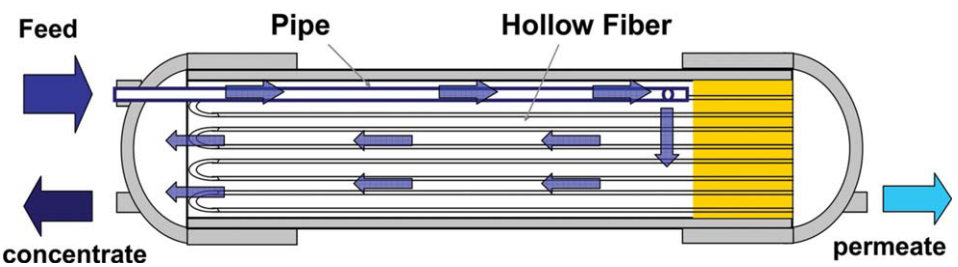

Figure 2 Schematic structure and flow pattern of typical axial flow type module. [Color figure can be viewed in the online issue, which is available at wileyonlinelibrary.com.]

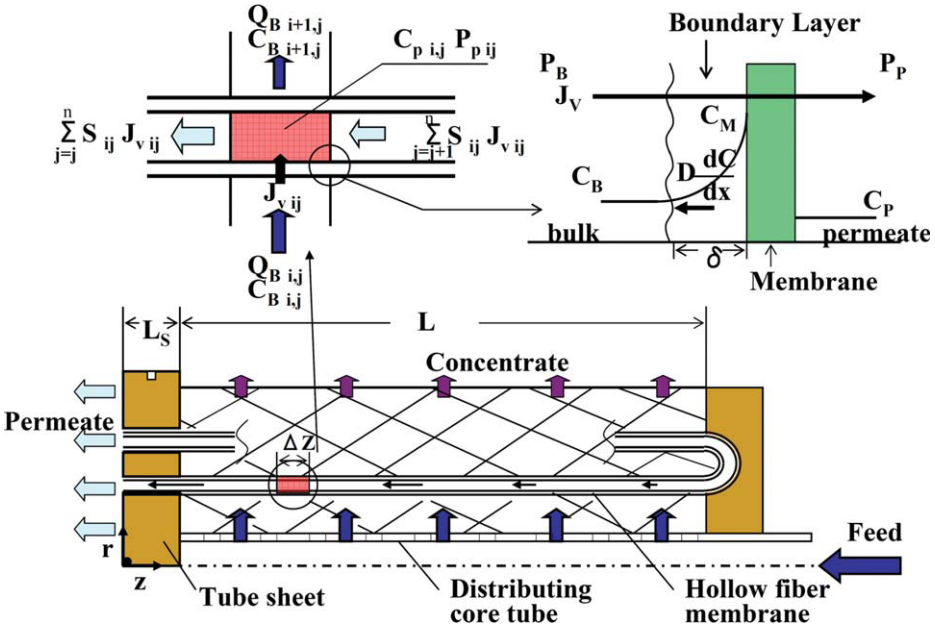

Figure 3 Schematic diagram of the FCP model in radial flow type module. [Color figure can be viewed in the online issue, which is available at wileyonlinelibrary.com.]

equation, which was derived for radial flow type hollow fiber RO membrane modules, with consideration of the radial and axial concentration profiles.[7]

$$Sh = 0.048Re^{0.6}\ Sc^{1/3} \tag{1}$$

Sh, *Re* and *Sc* are Sherwood number, Reynolds number, and Schmidt number, respectively.

The previous analytical (FCP) model on axial flow hollow fiber RO membrane module was conducted at much lower packing density (1%) of hollow fibers than the practical packing density (>50%) and neglected the axial concentration profile in the module. Under these conditions, the following dimensionless equation for mass transfer correlation was derived.[9]

$$Sh = 0.20Re^{0.6}\ Sc^{1/3} \tag{2}$$

The solution-diffusion model is based on the following membrane permeation equations:[10]

$$\mathrm{Jw} = A(\Delta P - \Delta\Pi) \tag{3}$$

$$\mathrm{Js} = B\Delta C \tag{4}$$

Jw, Js, *A*, *B*, ΔP, $\Delta\Pi$, and ΔC represent water flux through membrane, solute flux through membrane, pure water permeability coefficient, solute transport coefficient, pressure difference, osmotic pressure difference, and concentration difference, respectively.

Solutes accumulated on the membrane surface gradually develop a concentration polarization layer. The material balance in the layer is described by[10]

$$(C_M - C_P)/(C_B - C_P) = \exp(J_V/k) \tag{5}$$

where

$$J_V = (J_W + J_S)/\rho_p \tag{6}$$

$$C_P = J_S/J_V \tag{7}$$

C_M, C_P, and C_B represent concentrations at membrane surface, in permeated water and in bulk water, respectively. *k*, J_v and ρ_p are mass transfer coefficient, solution flux through membrane and density of permeate, respectively.

The pressure drop inside the fiber is expressed by the Hagen–Poiseuille equation:

$$\frac{dP}{dz} = \frac{128\mu_p Q_P}{\pi d_I^4} \tag{8}$$

P, Q_P, and μ_p represent pressure, flow rate and viscosity of permeated water, respectively. z is the axial coordinate, which means axial direction of the hollow fiber bundle as shown in Figure 4 and d_I represents the inner diameter of the hollow fiber.

The material balance within a fiber is given by:

$$\frac{dQ_P}{dz} = \pi d_O J_V, \quad L_S \le z \le L_S + L \tag{9}$$

where d_O, Ls, and *L* represent outer diameter of the hollow fiber, length of hollow fiber submerged in tube sheet, and effective length of hollow fiber in a bundle, respectively.

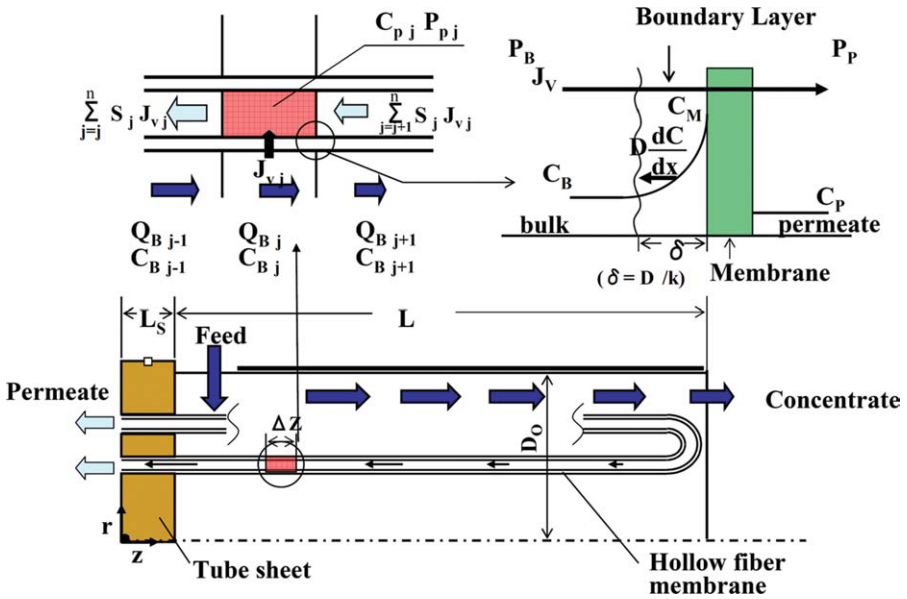

Figure 4 Schematic diagram of the FCP model in axial flow type module. [Color figure can be viewed in the online issue, which is available at wileyonlinelibrary.com.]

Differentiation of eq. (8) and substitution into eq. (9) gives the following equation.

$$\frac{d^2P}{dz^2} = \frac{128\mu_p}{d_I^4} d_O J_V \tag{10}$$

The material balance in the hollow fiber bundle is given by

$$\frac{dQ_B}{dz} = -\pi/4 D_O^2 (1-\sigma) J_V \zeta \; 0 \le r \le D_O/2 \tag{11}$$

$$\frac{d(Q_B C_B)}{dz} = -\pi/4 D_O^2 (1-\sigma) J_V C_P \zeta \; 0 \le r \le D_O/2 \tag{12}$$

where σ is packing density of fiber bundle. ζ and Q_B represent the membrane surface area per unit volume and flow rate of bulk water, respectively.

In the module, membrane area can be expressed by:

$$\mathrm{dS} = \pi d_O \mathrm{N dz} \tag{13}$$

where S and N represent surface area of membrane and number of hollow fibers in bundle, respectively.

Numerical analysis

The 12 equations from (2) to (13) were simultaneously solved using the finite difference method. The axial direction of the hollow fiber bundle (z-direction) was divided into "n" segments. In this analysis, numerical analysis was conducted by ignoring concentration profiles in the radial direction. However, the axial concentration profile was considered.

An axial flow type module is divided into two types, co-current and countercurrent. In this calculation, the counter-current type module was analyzed. A schematic diagram of the FCP model for axial counter-current flow is shown in Figure 4.

Equations (3) and (4) are developed as the following equations:

$$\begin{aligned} J_W &= A[(P_B - P_P) - (\Pi_M - \Pi_P)] \\ &= A[(P_B - P_P) - \alpha\Phi(C_B - C_P)] \end{aligned} \tag{14}$$

$$\begin{aligned} J_S &= B(C_M - C_P) \\ &= B\Phi(C_B - C_P) \end{aligned} \tag{15}$$

where

$$\Pi = \alpha C \tag{16}$$

$$\Phi = (C_M - C_P)/(C_B - C_P) \tag{17}$$

α and Φ represent osmotic pressure proportionality constant and concentration polarization coefficient, respectively. The membrane permeation flux J_{Vj} in the Δz region (j-th component) of the hollow fiber is expressed by the following equation.

$$\begin{aligned} J_{Vj} &= (J_{Wj} + J_{Sj})/\rho_{Pj} \\ &= A[(P_{Bj} - P_{Pj}) - (\alpha A - B)\Phi_j(C_{Bj} - C_{Pj})]/\rho_{Pj} \end{aligned} \tag{18}$$

The concentration polarization coefficient factor Φ_j is expressed by the following equation.

$$\Phi_j = exp(J_{Vj}/k_j) \tag{19}$$

The solute concentration in the permeate is expressed by the equation

$$C_{Pj} = J_{Sj}/J_{Vj} = J_{Sj}\rho_{Pj}/(J_{Wj} + J_{Sj}) \tag{20}$$

The pressure inside the hollow fiber, P_{Pj}, is obtained from the following equation derived from eqs. (8) and (9)

$$P_{Pj} - P_{Pj-1} = \frac{128\mu_{Pj}\Delta z^2 d_O}{d_I^4}\sum_{j=j}^{n} J_{Vj} \tag{21}$$

In the tube sheet of RO membrane element, the following equation is applied because there is no permeation in this region.

$$P_{P1} - P_0 = \frac{128\mu_{Pj}L_S\Delta z d_O}{d_{I_S}^4}\sum_{j=1}^{n} J_{Vj} \tag{22}$$

d_{Is} is the inner diameter of hollow fiber in the tube sheet, and P_0 is the pressure of permeated fluid at the open-ended position of the hollow fiber element.

The following mass balance equations are derived from eqs. (11) and (12)

$$Q_{Bj+1} = Q_{Bj} - S_j J_{Vj} \tag{23}$$

$$C_{Bj+1}Q_{Bj+1} = C_{Bj}Q_{Bj} - S_j C_{Pj} J_{Vj} \tag{24}$$

The membrane surface area S_j in the j-th component is derived from eq. (13).

$$S_j = \pi L d_O N/n \tag{25}$$

Calculation method

Hollow fiber properties (A, B, d_I, d_{IS}, d_O), hollow fiber bundle dimensions (D_O, L, L_S, N), properties of RO operation conditions (P_F, Rc, T_F) and the feed solution (C_F, D, μ, ρ) are known before calculation. eqs. (14), (15), and (18–22) were solved by convergence calculation through the axial direction of the hollow fiber bundle (z-direction) divided into "n" segments, because J_V, k, and Φ are linked with each other.

After calculation up to $j = n$, the overall flow rate and solute concentration are obtained by summing J_{Vj}, C_{Pj} and S_j.

$$Q_{PT} = \sum_{j=1}^{n} (J_{Vj}S_j) \tag{26}$$

$$C_{PT} = \left\{\sum_{j=1}^{n} (C_{Pj}J_{Vj}S_j)\right\}/Q_{PT} \tag{27}$$

A computer calculation flow chart for obtaining Q_{PT} and C_{PT} is shown in Figure 5. The simulation starts with the calculation on the feed solution inlet in the axial direction. The calculation was started from the fiber opening end to the end of fiber bundle. The iteration proceeds by changing the initial pressure at the fiber bundle end until the calculated pressure at that end becomes the same as the permeate outlet pressure.

In the calculation of each segment, Φ_j and C_{Bj} were initially assumed before calculating J_{Vj}, k_j, Φ_j and C_{Bj}. This calculation was repeated until the assumed Φ_j, C_{Bj} values were equal to the calculated values. Thus, J_{Vj} ,C_{Pj} and P_{Pj} were finally given for one segment. Then the calculation was done for the next segment in the axial direction. The calculation is advanced mesh by mesh to the concentrate outlet in the axial coordination, and J_{Vj} and C_{Pj} in each segment are determined.

As the number of segments n is increased, outlet values will be more accurate but calculation time will be longer. The value for n increased until the convergence value within 0.2% was obtained.

Q_{PT} and C_{PT} were obtained by eqs. (26) and (27) Then the recovery ratio defined as the ratio ofQ_{PT} to Q_F was obtained. The calculation was repeated until the initially assumed recovery ratio.

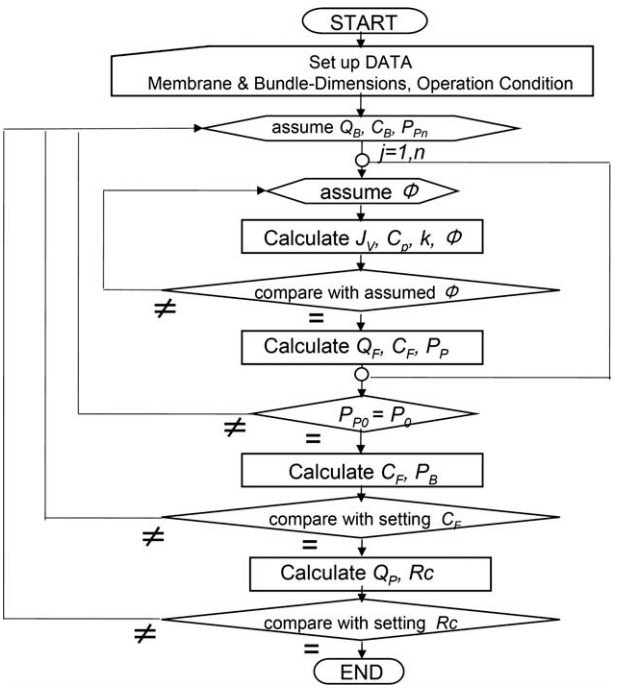

Figure 5 Computer flow diagram for the analytical method.

TABLE I
Characteristics of Hollow Fiber Membranes

d_O	175×10^{-6} (m)
d_I	85×10^{-6} (m)
A	1.1×10^{-9} (kg m^{-2} s^{-1} Pa^{-1})
B	1.8×10^{-8} (m/s)

EXPERIMENT

Permeability coefficients of hollow fiber membrane

The hollow fiber, with outer diameter 175 μm, was made from cellulose triacetate. The permeability coefficients A and B of the hollow fiber membrane were determined experimentally. A 1 m long U shaped small fiber bundle, made of several hundred hollow fibers, was installed in a one inch diameter pressure vessel. In this experiment, the feed velocity was greater than 5×10^{-2} m s^{-1}; the permeate flow rate and salt rejection did not depend on the velocity because no concentration polarization was generated. Coefficients A and B were determined by extrapolating the data to the point where the pressure drop inside the fiber was assumed to be zero. The A and B values obtained are given in Table I together with values of d_O and d_I.

Hollow fiber membrane module

The hollow fiber membrane module (Fig. 2) used in the experiment was the axial flow type (HK2105; Toyobo Co). In this module the feed solution flows parallel to the axial direction of the hollow fiber from the fiber opening end to the end of the fiber bundle for counter-current flow. The characteristics and geometric specifications of the hollow fiber modules are given in Table II. d_h shown in the Table is an equivalent hydraulic diameter and will be defined in eq. (29) later.

For the desalination experiments, the feed solution was an aqueous sodium chloride solution with concentration 0.5 kg m^{-3}. The applied pressure ranged from 0.29 to 0.49 MPa. The recovery ratio was 20 to 60%; the feed solution temperature was 298 K.

TABLE II
Characteristics and Geometric Specifications of Hollow Fiber Modules (HK2105)

D_O	0.051 (m)
L	0.245 (m)
L_S	0.034 (m)
d_h	12.35×10^{-3} (m)
N	43,200(−)
Σ	0.51(−)

RESULTS AND DISCUSSION

Mass transfer coefficient

Sekino and Fujiwara (1991) analyzed the experimental data of 8-in. diameter hollow fiber modules of radial flow type, and presented the mass transfer coefficient correlation equation as described above. In addition, Sekino (1995) analyzed the experimental data of very low packing density hollow fiber modules of axial flow type neglecting the axial solute concentration profile in the module, and obtained the correlation equation for the mass transfer coefficient. In other work, mass transfer correlation equations were reported for liquid–liquid contactors using hollow fiber membranes.[11] Prasad and Sirkar (1988) obtained shell-side mass transfer correlation equations for membrane extractors in axial flow, using xylene and water with acetic acid and packing densities of hollow fibers from 4 to 40%.

With these correlation equations as a guide, in this study the correlation as $ShSc^{-1/3}$ versus Re was obtained based on the performance data of the axial flow type module with high packing density in two pressure cases with considering the axial solute concentration profile in the module. A mass transfer coefficient was obtained by a trial and error method in which the estimated module performance by the analytical model discussed above agreed with experimental data. Here the mass transfer coefficient was a local value and was calculated in each segment in the module.

The relationship between $ShSc^{-1/3}$ and Re is shown in Figure 6. In this figure, Re shows the value calculated by mean of bulk flow rate in the module. $ShSc^{-1/3}$ shows the value obtained by mass transfer coefficient corresponding to mean of bulk flow rate in the module at each experiment condition. The correlation equation for the data is expressed as follows.

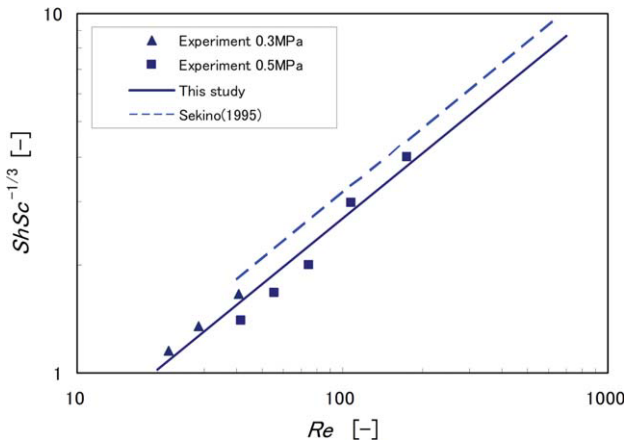

Figure 6 Correlation of mass transfer coefficient in axial flow module. [Color figure can be viewed in the online issue, which is available at wileyonlinelibrary.com.]

TABLE III
Correlation Equations for Mass Transfer Coefficient in Axial Flow Modules

System		Reverse osmosis	Reverse osmosis	Liauid extraction (Liquid–Liquid)
Authors		Sekino (1995)[9]	This study	Prasada and Sirkar (1998)[11]
Correlations		$Sh = 0.20Re^{0.6}Sc^{1/3}$	$Sh = 0.17Re^{0.6}Sc^{1/3}$	$Sh = 5.85(1 - \sigma)(d_h/L)Re^{0.6}Sc^{1/3}$
Flow range		$40 < Re < 1000$	$20 < Re < 200$	$0 < Re < 500$
Fluids	Inner side	permeate	permeate	acetic acid, etc
	Outer side	NaCl solution	NaCl solution	xylene, etc
Module type		RO mini-fiber modules	Toyobo RO module	Handmade extractor
Membrane materials		Cellulose triacetate	Cellulose triacetate	Polypropylene, etc
Packing density (%)		1	51	4–40

$$Sh = 0.17Re^{0.6}Sc^{1/3} \tag{28}$$

Here, the characteristic length in the Reynolds and Sherwood numbers was not the outer diameter of hollow fiber, but an equivalent hydraulic diameter d_h defined by the following equation.

$$d_h = 4(\text{cross} - \text{sectional area of flow})/\text{wetted perimeter} \tag{29}$$

Although the powers of the Reynolds and Sherwood numbers in eqs. (1), (2), and (28) are the same, the constants on the right side of the equations are different. In Figure 6, the results from eq. (2) obtained by Sekino[9] are shown by the dotted line. These results are a little higher than the experimental data.

The constant on the right side of the mass transfer correlation equation depends on the module structure, packing density of hollow fibers, fluid flow patterns and analytical model. In particular, the packing density of hollow fibers can be one of the most influential factors. When the packing density is very low, the hollow fiber module may have sufficient spaces among the hollow fibers for the feed solutions to be distributed uniformly to almost all of the membrane surfaces. On the contrary, if the packing density is very high all membrane surface areas cannot be utilized effectively. When the flux is evaluated as permeated mass volume divided by the geometrical membrane area, it will be smaller than the actual flux. Hence, the calculated mass transfer coefficient is lower than the intrinsic value in the high packing condition.

In addition, in the case of high packing density of hollow fibers, especially in a practical module, several hollow fibers compose a fiber group and the mass transfer occurs in two stages. One is the mass transfer around the fiber groups, and the other is that among the fiber groups.[12] Thus, the constant on the right side of the mass transfer correlation equation becomes smaller because mass transfer cannot occur sufficiently among the fiber groups. For these reasons, the constant in eq. (28) is smaller than that in eq. (2).

Prasad et al. showed the correlation of mass transfer coefficient for the axial flow module with various packing densities, although mass transfer was not considered for RO membrane but for liquid extraction. In addition, they derived a mass transfer correlation equation that depended on the packing density of hollow fibers, σ, as shown in Table III. Figure 7 shows a comparison of the correlations as $ShSc^{-1/3}$ versus Re by three mass transfer correlation equations for the axial flow module in the conditions of module dimensions and operation for this study. The mass transfer coefficients obtained in this study are between the data from the equation of Sekino et al. and those of Prasad et al.

In this work, the concentration profile of NaCl in the axial direction was considered. Figure 8 shows the calculated results of C_F and C_P changes against the axial distance. The C_F and C_P values increased with the increase of the axial distance. In addition, when the recovery ratio Rc is high, the increases of C_F and C_P became more pronounced.

Module performance and verification of the model

The usefulness of the analytical model presented here was verified by comparison with the

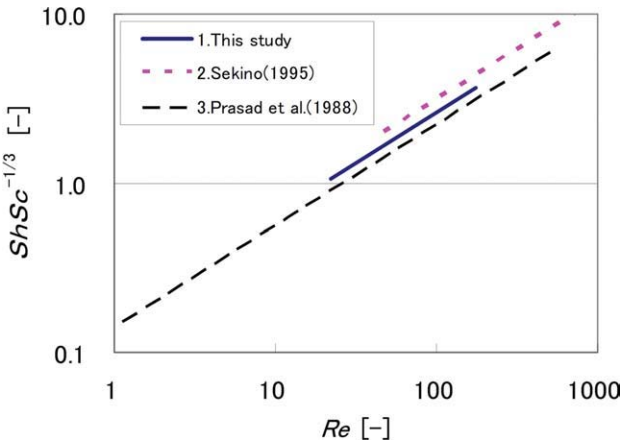

Figure 7 Comparison of mass transfer coefficients by three correlation equations. [Color figure can be viewed in the online issue, which is available at wileyonlinelibrary.com.]

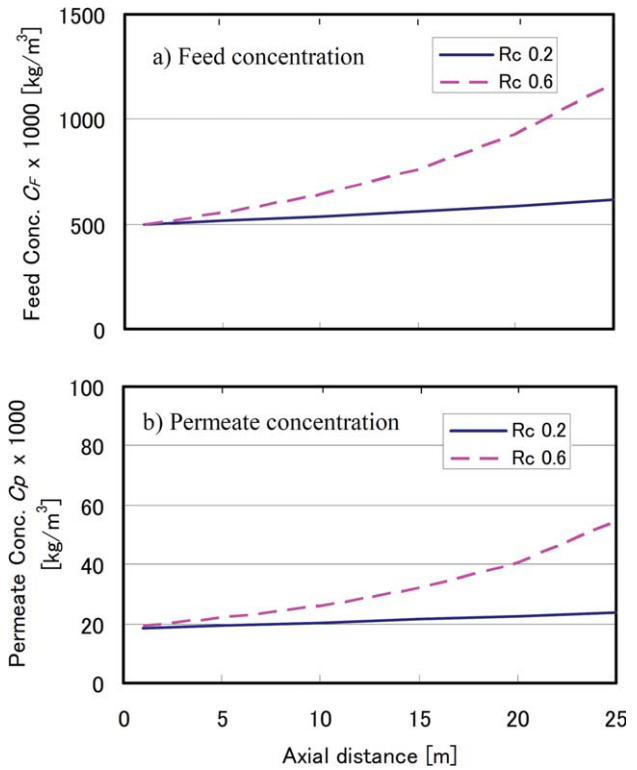

Figure 8 Relation between solute concentrations and axial distance. (a) Feed concentration, (b) Permeate concentration. [Color figure can be viewed in the online issue, which is available at wileyonlinelibrary.com.]

experimental data for a 2-in. hollow fiber RO module (HK2105; Toyobo Co). The specifications of this module are given in Table II.

The flow rate of permeated water Q_p is plotted against recovery ratio Rc in Figure 9. The data in two cases with different applied pressures are included in this figure. The flow rate decreases slightly as the recovery ratio increases, because the solute concentration increases and solution velocity decreases in the module, as the recovery ratio increases. The results calculated by the model equations are shown in this figure as solid lines. The calculated results agreed well with the experimental data.

Figure 10 shows the relationship between the NaCl rejection R_j and R_c. The solute rejection decreases with increase of R_c because solute concentration increases and solution velocity decreases, as the recovery ratio increases (as for flow rate dependence on recovery ratio). The agreement between the calculated results and the experimental data was again satisfactory. Thus, the model derived in this work can be applied to analysis of an RO membrane module of the axial flow type.

If the axial concentration profile is not considered in the FCP model, the module performances shown in Figures 9 and 10 cannot be calculated. For examples, when the feed solute concentration C_F is constant, the recovery ratio R_C becomes zero. The value of C_F must be increased in the case of increased R_C, as shown in Figure 8.

CONCLUSIONS

The FCP model was applied to analysis of a hollow fiber RO membrane module of the axial flow type. In this analysis, the axial solute concentration profile in the module was considered. The mass transfer correlation equation was derived for an axial flow type module with high packing density of hollow fibers. The calculated results for water flow rate and NaCl rejection agreed satisfactorily with experimental data. This model will be applied to the practical modules with a high packing density.

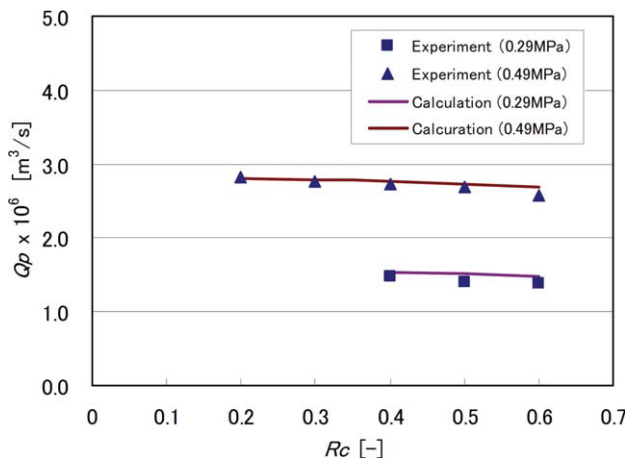

Figure 9 Relation between flow rate of permeated water and recovery ratio. [Color figure can be viewed in the online issue, which is available at wileyonlinelibrary.com.]

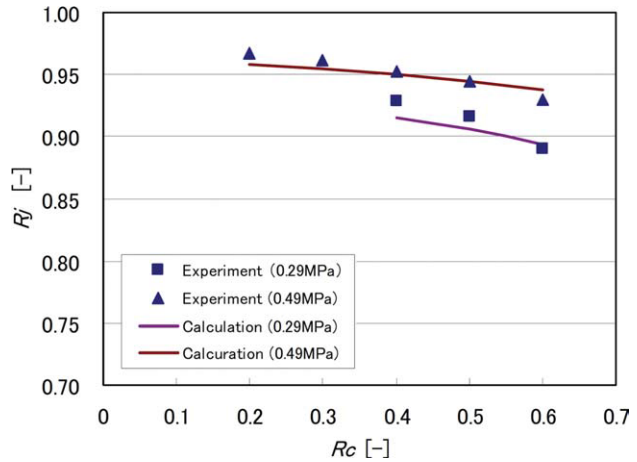

Figure 10 Relation between NaCl rejection and recovery ratio. [Color figure can be viewed in the online issue, which is available at wileyonlinelibrary.com.]

NOMENCLATURE

A	pure water permeability coefficient ($kg'm^{-2'}s^{-1'}Pa^{-1}$)
B	solute transport coefficient (m/s)
C	solute concentration (kg/m^3)
D_O	outer diameter of fiber bundle (m)
D	diffusion coefficient (m^2/ s)
d_h	hydraulic diameter defined by Eq. (29) (m)
d_I	inner diameter of hollow fiber (m)
$d_{I\ s}$	inner diameter of hollow fiber at tube sheet (m)
d_O	outer diameter of hollow fiber (m)
Js	solute flux through membrane ($kg'm^{-2}$ s^{-1})
J_V	solution flux through membrane ($m^{3'}m^{-2'}$ s^{-1})
J_W	water flux through membrane ($kg'm^{-2'}$ s^{-1})
k	mass transfer coefficient (m/s)
L	effective length of hollow fiber in bundle (m)
L_S	length of hollow fiber submerged in tube sheet (m)
N	number of hollow fibers in bundle (-)
P	pressure (Pa)
P_0	pressure of permeate at exit (Pa)
Q	flow rate (m^3/s)
R_c	recovery ratio, Q_P/Q_F (-)
R_e	Reynolds number, $doV\rho/\mu$ or $d_hV\rho/\mu$ (-)
R_j	rejection, (1-C_P/C_F) (-)
S	surface area (m^2)
Sc	Schmidt number, $\mu/\rho D$ (-)
Sh	Sherwood number, kdo/D or kd_h/D (-)
T	temperature (K)
V	fluid velocity (m/s)
65370	axial coordinate (m)

Greek letters

α	osmotic pressure proportionary constant ($Pa/(kg/m^3)$)
Δ	difference (-)
ζ	membrane area per unit volume (1/m)
μ	viscosity (Pa s)
ρ	density (kg/m^3)
σ	packing density of fiber bundle (-)
Φ	concentration polarization coefficient (-)

Subscripts

B	bulk (shell side)
F	feed (shell side)
j	j-th component at axial coordinate
M	membrane surface
P	permeate (bore side)
S	solute
T	total
t	tube value

References

1. Li N. N.; Fane G. A.; Winston Ho, S. W.; Matsuura, T.; Adv Mem Technol Appl; Wiley: Hoboken, 2008, Chap. 2.
2. Baker, R. W. Mem Technol Appl, 2th ed; Wiely: Chichester, 2004, Chap. 3.
3. Gill, W. N.; Bansal B. AIChE J 1973, 19, 823.
4. Dandavati, M. S.; Doshi M. R.; Gill W.N. Chem Eng Sci 1975, 30, 877.
5. Kabadi, V. N.; Doshi M. R.; Gill, W, M. Chem Eng Commun 1979, 3, 339.
6. Ohya, H.; Nakajima, H.; Takagi, K.; Kagawa S.; Negishi, Y. Desalination 1977, 21, 257.
7. Sekino, M.; Fujiwara N. Kagaku Kogaku Ronbunshu 1991, 17, 1088.
8. Sekino, M. J Membr Sci 1993, 85, 241.
9. Sekino, M. J Chem Eng Jpn 1995, 28, 843.
10. Kimura, S.; Sourirajan S. AIChE J 1967, 13, 497.
11. Prasad, R.; Sirkar, K. K. AIChE J 1988, 34, 177.
12. Kumano, A.; Sekino, M.; Mtasui, Y.; Fujiwara, N.; Matsuyama H. J Membr Sci 2008, 324, 136.